Discord and information deficit in the *XX* chain

L. Ciliberti, N. Canosa, and R. Rossignoli
Departamento de Física-IFLP, Universidad Nacional de La Plata, C.C. 67, La Plata (1900), Argentina
(Received 10 January 2013; published 22 July 2013)

We examine the quantum correlations of spin pairs in the cyclic *XX* spin-1/2 chain in a transverse field through the analysis of the quantum discord, the geometric discord, and the information deficit. It is shown that while these quantities provide the same qualitative information, being nonzero for all temperatures and separations and exhibiting the same type of asymptotic behavior for large temperatures or separations, important differences arise in the minimizing local measurement that defines them. Whereas the quantum discord prefers a spin measurement perpendicular to the transverse field, the geometric discord and information deficit exhibit a perpendicular-to-parallel transition as the field increases, which subsists at all temperatures and for all separations. Moreover, it is shown that such transition signals the change from a Bell state to an aligned separable state of the dominant eigenstate of the reduced density matrix of the pair. Full exact results for both the thermodynamic limit and the finite chain are provided through the Jordan-Wigner fermionization.

DOI: 10.1103/PhysRevA.88.012119 PACS number(s): 03.65.Ud, 03.67.Mn, 75.10.Pq

I. INTRODUCTION

The investigation of quantum correlations in mixed states is presently attracting strong attention [1]. While in bipartite pure states such correlations can be identified with entanglement, it was recently recognized that separable (nonentangled) bipartite mixed states, defined as states which can be created by local operations and classical communication, and which are therefore convex mixtures of product states [2], may still exhibit useful quantum correlations, stemming from the noncommutativity of the different products. The mixed-state-based quantum algorithm introduced by Knill and Laflamme (KL) [3] has shown that an exponential speedup over classical algorithms can in fact be achieved without entanglement [4], in contrast with the case of pure states [5].

This has turned the attention to alternative measures of quantum correlations for mixed states, such as the quantum discord [1,6–8], which are able to capture the quantumness of such mixed states, vanishing just for states diagonal in a product basis and coinciding with entanglement in the pure state limit. A finite discord between the control qubit and the remaining maximally mixed qubits was in fact found in the KL algorithm [9], renewing the interest on this measure [10–14]. Other measures with similar properties include the closely related one-way information deficit [1,15,16], the geometric discord [17], which allows an easier evaluation, and the generalized entropic measures of Ref. [18], which include the previous ones as particular cases. Various applications and operational interpretations of the quantum discord and related measures were recently provided [1,10,16,19–24]. We remark that all these measures require a minimization over local measurements in one of the constituents (which can be viewed as the determination of the least disturbing local measurement [25]), which makes their evaluation difficult in systems with high dimensionality.

Spin chains provide an interesting scenario for studying these measures and their relation with criticality [1,26–36]. In particular, the state of a spin pair in an entangled ground state (GS) is in general a mixed state, entailing that differences between the entanglement and the quantum discord of a spin pair will arise already at zero temperature [26,28,30]. These differences become significant in the exact ground states of finite *XY* chains for transverse fields lower than the critical field B_c [30], with the quantum discord reaching full range in this region.

The aim of this work is to analyze in detail the behavior of the quantum discord, the geometric discord, and the one-way information deficit of spin pairs in chains with *XX*-type first-neighbor couplings in a transverse field, at both zero and finite temperatures. Such a model is particularly interesting for both quantum information and condensed matter physics, exhibiting distinct features such as eigenstates with definite magnetization along the field axis and a special critical behavior [37]. It is first shown that in contrast with entanglement [38–40], discord-type measures exhibit common features such as a nonzero value for all separations L at all temperatures $T > 0$. Exact asymptotic expressions for the decay with L and T will be provided on the basis of the exact treatment based on the Jordan-Wigner fermionization [39–42]. Nonetheless, we will also show that important differences between the quantum discord on the one side and the geometric discord and information deficit on the other side do arise in the minimizing local spin measurement. While in the quantum discord the latter is always orthogonal to the transverse field (even at strong fields if $T > 0$), in the geometric discord and information deficit it exhibits a perpendicular-to-parallel transition as the field increases, at a field lower than the $T = 0$ critical field B_c. Such transition in the minimizing measurement is present at all temperatures and separations, and, as will be shown, is a signature of the transition from a Bell state to a separable aligned state of the dominant eigenstate of the reduced density matrix of the pair. This difference indicates a distinct response of the minimizing measurement in these quantities to the onset of quantum correlations.

In Sec. II, we summarize the main features of the previous measures, including the equations that determine the stationary local measurements. The application to the spin-1/2 *XX* chain is made in Sec. III, where we first discuss some general properties of these measures in this model and show that spin measurements parallel and perpendicular to the field are always stationary. We then consider in detail the

thermodynamic limit and the finite case. Details of the exact calculation are provided in the Appendix. Conclusions are finally given in Sec. IV.

II. DISCORD AND GENERALIZED INFORMATION DEFICIT

Let us consider a bipartite quantum system $A + B$ initially in a state ρ_{AB}. A local complete projective measurement M_B on system B is defined by a set of orthogonal projectors $\Pi_j^B = I_A \otimes \Pi_j$, where $\Pi_j = |j_B\rangle\langle j_B|$ are one-dimensional projectors satisfying $\sum_j \Pi_j = I_B$, $\Pi_j \Pi_k = \delta_{jk}\Pi_k$. The state of the total system after an unread measurement of this type becomes

$$\rho'_{AB} = \sum_j \Pi_j^B \rho_{AB} \Pi_j^B. \tag{1}$$

In [18,25] we considered the *minimum generalized information loss* by such measurement,

$$I_f^B = \operatorname*{Min}_{M_B} S_f(\rho'_{AB}) - S_f(\rho_{AB}), \tag{2}$$

where $S_f(\rho) = \operatorname{Tr} f(\rho)$ denotes a general entropic form, with f a smooth strictly concave function for $p \in [0,1]$, satisfying $f(0) = f(1) = 0$ [43]. Equation (2) satisfies $I_f^B \geqslant 0$ for any such f, becoming the generalized entanglement entropy $S_f(\rho_B) = S_f(\rho_A)$ in the case of pure states ($\rho_{AB}^2 = \rho_{AB}$). However, it can be nonzero in separable *mixed* states, vanishing just for states which are already of the form (1) [18], i.e., states which remain unchanged after the local measurement M_B and are hence diagonal in a product basis $\{|i_{j_A}\rangle \otimes |j_B\rangle\}$. The positivity of $I_f^B \; \forall S_f$ follows from the majorization relation $\rho'_{AB} \prec \rho_{AB}$ satisfied by (1) [18,25,44].

If $f(\rho) = -\rho \log_2 \rho$, $S_f(\rho)$ becomes the von Neumann entropy $S(\rho)$ and Eq. (2) becomes the *one-way information deficit* [1,15,16], which we will denote as I_1^B. It can be rewritten in terms of the relative entropy [44,45] $S(\rho \parallel \rho') = -\operatorname{Tr} \rho(\log_2 \rho' - \log_2 \rho)$ as [18]

$$I_1^B = \operatorname*{Min}_{M_B} S(\rho'_{AB}) - S(\rho_{AB}) = \operatorname*{Min}_{M_B} S(\rho_{AB} \parallel \rho'_{AB}). \tag{3}$$

For a pure state, I_1^B becomes the standard entanglement entropy $S(\rho_A) = S(\rho_B)$.

If $f(\rho) = 2\rho(1-\rho)$, $S_f(\rho)$ becomes the so-called *linear entropy* $S_2(\rho) = 2(1 - \operatorname{Tr} \rho^2)$ and Eq. (2) becomes

$$I_2^B = 2 \operatorname*{Min}_{M_B} \operatorname{Tr}\left(\rho_{AB}^2 - {\rho'}_{AB}^2\right) = 2 \operatorname*{Min}_{\rho'_{AB}} ||\rho_{AB} - \rho'_{AB}||^2, \tag{4}$$

where $||O||^2 = \operatorname{Tr} O^\dagger O$ and the last minimization can be extended to any state of the general form (1). It is then seen that (4) is proportional to the *geometric discord* introduced in [17], defined as the square of the minimum Hilbert-Schmidt distance from ρ_{AB} to a classically correlated state with respect to B. For pure states, I_2^B becomes the squared concurrence C_{AB}^2 [46], which for such states is just the linear entropy of any of the subsystems [47].

Both measures (3) and (4) can then be regarded as particular cases of the generalized information deficit (2). We may similarly define [25] $I_q^B = S_q(\rho'_{AB}) - S_q(\rho_{AB})$ for entropies $S_q(\rho)$ associated to $f(\rho) = (\rho - \rho^q)/(1 - 2^{1-q})$, $q > 0$ [48]. I_q^B reduces to (4) for $q = 2$ and to (3) for $q \to 1$ [$S_q(\rho) \to S(\rho)$ in this limit]. Normalization of $f(\rho)$ was chosen such that $I_f^B = 1 \; \forall \, S_f$ for a two-qubit Bell state.

On the other hand, the quantum discord [6,7] for a measurement in B can be written as

$$\begin{aligned} D^B &= \operatorname*{Min}_{M_B} S(A|M_B) - S(A|B) \\ &= \operatorname*{Min}_{M_B} \left[I_1^{M_B}(\rho_{AB}) - I_1^{M_B}(\rho_B)\right], \end{aligned} \tag{5}$$

where $S(A|M_B)$ denotes the conditional von Neumann entropy of A given a measurement M_B in B, $S(A|B) = S(\rho_{AB}) - S(\rho_B)$ is the quantum conditional entropy, and the last expression (5) is the result for a complete projective measurement M_B, which is the case we will here consider. D^B is just the minimum decrease of the *mutual information* $S(A) - S(A|B)$ after an unread measurement in B [6,7]. We then have $D^B \leqslant I_1^B$, with $D^B = I_1^B$ when the minimizing measurements for D^B and I_1^B coincide and $\rho'_B = \rho_B$. Nonetheless, like I_1^B, $D^B \geqslant 0$, vanishing just for the classically correlated states (1) and reducing to the entanglement entropy $S(\rho_A) = S(\rho_B)$ for pure states ρ_{AB}.

However, important differences between I_1^B (or in general I_f^B) and D^B may arise in the minimizing measurement. While for a general classically correlated state of the form (1) the minimum (0) for *both* D^B and *all* I_f^B is attained for a measurement in the local basis defined by the projectors Π_j^B (i.e., the pointer basis [6,7]), in the particular case of product states $\rho_A \otimes \rho_B$, D^B (but not I_f^B) becomes the same for *any* M_B, as for such states $S(A|M_B) = S(A) \; \forall \; M_B$. The same holds for pure states ρ_{AB}, where D^B is again the same for any M_B, as here $S(A|M_B) = 0 \; \forall M_B$ of the present form, whereas the minimum I_f^B is obtained, for *any* S_f, for a measurement M_B in the local part of the Schmidt basis [18], i.e., again in the basis of eigenstates of the reduced state ρ_B. These differences will have important consequences for the results of the next section, leading to a quite different response of the minimizing measurement to the onset of quantum correlations. They reflect the fact that while in I_f^B one is looking for the least disturbing local measurement, such that ρ'_{AB} is as close as possible to ρ_{AB}, in D^B the search is for the measurement in B which makes the ensuing conditional entropy smallest, i.e., by which one can learn the most about A.

We also remark that the determination of the minimizing measurement M_B is in general a difficult problem. Complete projective measurements at B are determined by $d_B^2 - d_B$ real parameters if B has a Hilbert space of dimension d_B, growing then exponentially with the number of components of B. For I_f^B, the minimizing measurement should fulfill the stationary condition [25,49]

$$\operatorname{Tr}_A[f'(\rho'_{AB}), \rho_{AB}] = 0, \tag{6}$$

which leads to $d_B(d_B - 1)$ real equations [25]. In the quantum discord (5), an additional term $-[f'(\rho'_B), \rho_B]$ is to be added in (6), with $f(\rho) = -\rho \log_2 \rho$ [25] (see also [50,51]).

Nevertheless, in the case of the geometric discord I_2, the final equations can be simplified considerably. In particular, for a general mixed state of two qubits

$$\rho_{AB} = \tfrac{1}{4}\left(I + \boldsymbol{r}_A \cdot \boldsymbol{\sigma}_A + \boldsymbol{r}_B \cdot \boldsymbol{\sigma}_B + \boldsymbol{\sigma}_A^t J \boldsymbol{\sigma}_B\right), \tag{7}$$

where $\boldsymbol{\sigma} = 2\boldsymbol{s}$ are the Pauli matrices, $\boldsymbol{\sigma}_A = \boldsymbol{\sigma} \otimes I$, $\boldsymbol{\sigma}_B = I \otimes \boldsymbol{\sigma}$, $\boldsymbol{r}_{A,B} = \langle \boldsymbol{\sigma}_{A,B} \rangle$ and $J = \langle \boldsymbol{\sigma}_A \boldsymbol{\sigma}_B^t \rangle$, it can be shown that [17]

$$I_2^B = \tfrac{1}{2}(\mathrm{tr}\, M_2 - \lambda_1), \tag{8}$$

where λ_1 is the largest eigenvalue of the positive-semidefinite 3×3 matrix $M_2 = \boldsymbol{r}_B \boldsymbol{r}_B^t + J^t J$. The minimizing M_B is a spin measurement along the direction of the associated eigenvector $\boldsymbol{k}_1$ of M_2. A closed expression for I_3^B can also be obtained for this case [25].

III. APPLICATION TO THE *XX* MODEL

We now consider a chain of N spins $\boldsymbol{s}_i$ with first-neighbor *XX* couplings in a uniform transverse magnetic field. The Hamiltonian reads as

$$H = \sum_i B s_{iz} - J(s_{ix}s_{i+1,x} + s_{iy}s_{i+1,y}), \tag{9}$$

and is obviously invariant under rotations around the z axis, satisfying $[H, S_z] = 0$, with $S_z = \sum_i s_{iz}$ the z component of total spin. Its eigenstates can then be characterized by the total magnetization M along z. The sign of the field B and the coupling strength J can be changed by local rotations $e^{i\pi s_{jz}}$ at all and even spins j, respectively (assuming N even in the cyclic case $N + 1 \equiv 1$), so that we will set in what follows $B \geqslant 0$, $J \geqslant 0$.

We will examine the spin-1/2 case, where exact results for finite N as well as the thermodynamic limit $N \to \infty$ can be obtained via the Jordan-Wigner fermionization (see Appendix). We will focus on the cyclic case $N + 1 \equiv 1$, where pair correlations between spins i and j in the ground state or in the thermal state $\rho \propto \exp[-\beta H]$ will depend just on the separation $L = |i - j|$.

For any global state ρ satisfying $[\rho, S_z] = 0$, the reduced state $\rho_{ij} = \mathrm{Tr}_{\overline{ij}}\, \rho$ of any pair $i \neq j$ will commute with $s_{iz} + s_{jz}$. In the cyclic case, $\rho_L \equiv \rho_{ij}$ will then have the form

$$\rho_L = \begin{pmatrix} p_L^+ & 0 & 0 & 0 \\ 0 & p_L & \alpha_L & 0 \\ 0 & \alpha_L & p_L & 0 \\ 0 & 0 & 0 & p_L^- \end{pmatrix} \tag{10}$$

$$= p_L^+ |\uparrow\uparrow\rangle\langle\uparrow\uparrow| + p_L^- |\downarrow\downarrow\rangle\langle\downarrow\downarrow| + (p_L + \alpha_L)|\Psi_+\rangle\langle\Psi_+| + (p_L - \alpha_L)|\Psi_-\rangle\langle\Psi_-|, \tag{11}$$

where (10) is the representation in the standard basis and (11) the eigenvector expansion, with $|\Psi_\pm\rangle = \frac{|\uparrow\downarrow\rangle \pm |\downarrow\uparrow\rangle}{\sqrt{2}}$ Bell states. Here, $p_L^+ + p_L^- + 2p_L = 1$, with

$$p_L^\pm = \tfrac{1}{4} \pm \langle s_z \rangle + \langle s_{iz} s_{jz} \rangle, \tag{12}$$

$$\alpha_L = \langle s_{ix} s_{jx} + s_{iy} s_{jy} \rangle, \tag{13}$$

and $\langle s_z \rangle = \langle S_z \rangle / N$ the intensive average magnetization along z. It corresponds to $\boldsymbol{r}_A = \boldsymbol{r}_B = (0,0,2\langle s_z \rangle)$ and $J_{\mu\nu} = \delta_{\mu\nu} J_\mu$ in (7), with $2\langle s_z \rangle = p_L^+ - p_L^-$, $J_x = J_y = 2\alpha_L$, $J_z = 1 - 4p_L$.

The eigenvectors of ρ_L in the ground or thermal state will not depend then on the field or separation. For $B \geqslant 0$ and $J \geqslant 0$ in (9), $p_L^- \geqslant p_L^+$ and $\alpha_L \geqslant 0$. The largest eigenvalue of ρ_L will then correspond to the Bell state $|\Psi_+\rangle$ if

$$\alpha_L > \alpha_L^c = p_L^- - p_L, \tag{14}$$

and to the aligned separable state $|\downarrow\downarrow\rangle$ if $\alpha_L < \alpha_L^c$. Hence, in the ground state we may expect as the field decreases a transition from $|\downarrow\downarrow\rangle$ to $|\Psi_+\rangle$ in the dominant eigenstate of ρ_L, at a certain field $B_c^L \leqslant B_c$, where $B_c = J$ denotes the $T = 0$ critical field [such that the ground state is fully aligned $(M = -N/2)$ for $B > B_c$]. We will see such crossing reflected in the transition exhibited by the geometric discord and the information deficit (but not the quantum discord). We will also find the same effect at finite temperatures.

A. Parallel and perpendicular geometric discord and information deficit

We first discuss the general properties of the discord and information deficit of the states (10). Due to the permutation symmetry of ρ_{ij}, we will omit in what follows the superscript B (i.e., j) in I_f and D, as $I_f^B = I_f^A$, $D^B = D^A$. For $\alpha_L = 0$, ρ_L is diagonal in the standard basis and will then have zero entanglement and discord: $E = D = I_f = 0 \;\forall\; S_f$. It will be, however, classically correlated, being a product state $\rho_i \otimes \rho_j$ only when $p_L = \sqrt{p_L^+ p_L^-}$ (in which case $\rho_i = \rho_j = \sqrt{p_L^+}|\uparrow\rangle\langle\uparrow| + \sqrt{p_L^-}|\downarrow\rangle\langle\downarrow|$).

Quantum correlations will then be driven solely by α_L, and will lead to a finite value of D and $I_f \;\forall\, \alpha_L \neq 0$. The geometric discord (4) for such state can be evaluated immediately with Eq. (8) [here $(M_2)_{\mu\nu} = \delta_{\mu\nu}\lambda_\mu$, with $\lambda_x = \lambda_y = J_x^2$, $\lambda_z = J_z^2 + |\boldsymbol{r}_B|^2$] and reads as

$$I_2 = \begin{cases} I_2^z = 4\alpha_L^2, & |\alpha_L| \leqslant \alpha_L^t \\ I_2^\perp = 2\left(\alpha_L^2 + {\alpha_L^t}^2\right), & |\alpha_L| \geqslant \alpha_L^t \end{cases} \tag{15}$$

where $\alpha_L^t = \frac{\sqrt{\lambda_z}}{2} = \sqrt{\frac{(p_L^- - p_L)^2 + (p_L - p_L^+)^2}{2}}$ and the superscript in I_2 indicates the direction of the minimizing local spin measurement (along z if $|\alpha_L| < \alpha_L^t$ and along any orthogonal direction $\boldsymbol{k}$ if $|\alpha_L| > \alpha_L^t$). Hence, I_2 increases first quadratically with α_L and exhibits then a parallel $\to$ perpendicular transition at $\alpha_L = \alpha_L^t$, corresponding to a transition field B_t^L. For $p_L^- > p_L$ such transition *correlates with that exhibited by the dominant eigenstate* of ρ_L [Eq. (14)]. In fact, if $|p_L^+ - p_L| = |p_L^- - p_L|$ and $p_L^- > p_L$, $\alpha_L^t = \alpha_L^c$.

Equation (15) is to be contrasted with the concurrence of ρ_L, which requires a finite threshold value of α_L:

$$C = 2\,\mathrm{Max}[|\alpha_L| - \sqrt{p_L^+ p_L^-}, 0]. \tag{16}$$

Hence, discord-type quantum correlations with zero entanglement will arise for $0 < |\alpha_L| \leqslant \sqrt{p_L^+ p_L^-}$.

The behavior of the generalized information deficit (2) is similar to that of the geometric discord. For a spin measurement along a vector $\boldsymbol{k}$ forming an angle γ with the z axis, the eigenvalues of the post-measurement state ρ_L' are, setting $\delta = \langle s_z \rangle = (p_L^+ - p_L^-)/2$ and $\mu, \nu = \pm 1$,

$$p'^{\nu}_{\mu} = \frac{1 + 2\nu\delta\cos\gamma + \mu\sqrt{[(1 - 4p_L)\cos\gamma + 2\nu\delta]^2 + 4\alpha_L^2 \sin^2\gamma}}{4}.$$

It is then verified that $\partial I_f^\gamma/\partial\gamma = 0$ at $\gamma = 0$ and $\pi/2$: *Both parallel ($\gamma = 0$) and perpendicular ($\gamma = \pi/2$) measurements are always stationary*, in agreement with the general considerations of [25]. Intermediate minima may also arise for a general S_f, but the essential competition is between $I_f^z \equiv I_f^0$ and $I_f^\perp \equiv I_f^{\pi/2}$.

For small α_L and $\delta \neq 0$, the minimum I_f^γ for any S_f will be obtained for $\gamma = 0$, with

$$I_f^z = 2f(p_L) - f(p_L + \alpha_L) - f(p_L - \alpha_L) \approx k_f \alpha_L^2, \quad (17)$$

where $k_f = |f''(p_L)|$ (we assumed here $p_L \neq 0$). Hence, as α_L increases from 0, all I_f will exhibit an initial *quadratic increase* with α_L, like the geometric discord.

On the other hand, if $\delta = 0$ ($p_L^+ = p_L^-$), as in the case of zero field in the ground or thermal state, the minimum I_f^γ for *any* S_f is attained for $\gamma = 0$ if $|\alpha_L| < \alpha_L^t$ and for $\gamma = \pi/2$ if $|\alpha_L| > \alpha_L^t$, where $\alpha_L^t = |\frac{1}{2} - 2p_L| = |p_L^- - p_L|$ as in Eq. (15). Hence, *all* I_f's will in this case exhibit, like the geometric discord, a parallel $\rightarrow$ perpendicular transition at the *same* value of α_L. Moreover, for $p_L^- > p_L$, α_L^t coincides in this case *exactly* with α_L^c, i.e, with the value where the dominant eigenstate of ρ_L becomes a Bell state.

The same behavior occurs when $p_L^\pm = \frac{1}{4} \pm \delta$ (implying $p_L = \frac{1}{4}$) with α_L, δ small, a typical situation to be encountered at high temperatures or large separations. A series expansion of I_f^γ leads to $I_f^\gamma \approx k_f[\alpha_L^2 - \frac{1}{2}\sin^2\gamma(\alpha_L^2 - \delta^2)]$, where $k_f = |f''(1/4)|$, implying again

$$I_f = \begin{cases} I_f^z \approx k_f\,\alpha_L^2, & |\alpha_L| < |\delta| \\ I_f^\perp \approx k_f\big(\alpha_L^2 + \delta^2\big)/2, & |\alpha_L| > |\delta| \end{cases} \quad (18)$$

with $\alpha_L^t = |\delta| = \alpha_L^c$ if $p_L^- > p_L$. Hence, we obtain in this case a universal parallel $\rightarrow$ transverse transition at $|\alpha_L| = |\delta|\ \forall\ S_f$ and L. In other words, all I_f behave like the geometric discord in this limit.

In contrast, the minimizing projective spin measurement of the quantum discord D will not exhibit such transition for the present Hamiltonian. We obtain, setting now $f(p) = -p\,\log_2 p$,

$$D^\gamma = I_1^\gamma - \sum_{\nu=\pm}\left[f\left(\frac{1}{2} + \nu\delta\cos\gamma\right) - f\left(\frac{1}{2} + \nu\delta\right)\right]. \quad (19)$$

Hence, $D^z \equiv D^0 = I_1^z$, but $D^\gamma < I_1^\gamma$ if $|\cos\gamma| < 1$ and $\delta \neq 0$ (however, at zero field, $\delta = 0$ and $D^\gamma = I_1^\gamma\ \forall\,\gamma$, implying $D = I_1$). While both $\gamma = 0$ and $\pi/2$ are again always stationary, the minimum D^γ will be always obtained for $\gamma = \pi/2$ ($D = D^\perp$) for the actual reduced states derived from the ground or thermal state determined by H, directly reflecting the spin-spin coupling in (9) (which involves the spin components perpendicular to the field axis). This will also occur for small α_L since in this limit the actual values of $p_L^\pm$ will correspond to a product state, entailing no preferred direction in D^γ for $\alpha_L = 0$. In fact, for small α_L and $\gamma = \pi/2$, Eq. (19) leads, for $p_L = \sqrt{p_L^+ p_L^-} > 0$, to

$$D^\perp \approx \frac{1}{\ln 2}\left(\frac{1}{p_L} - \frac{\operatorname{arctanh} 2\delta}{\delta}\right)\alpha_L^2, \quad (20)$$

which is always smaller than $D^z = I_f^z \approx \frac{\alpha_L^2}{p_L \ln 2}$. Nonetheless, a quadratic increase with α_L is also present.

B. Thermodynamic limit

We will first examine the previous quantities in the ground and thermal states of (9) in the large-N limit, where we may express all elements of ρ_L in terms of the integrals (see Appendix)

$$g_L = \frac{1}{\pi}\int_0^\pi \frac{\cos(L\omega)}{1 + e^{\beta(B - J\cos\omega)}}\,d\omega, \quad (21)$$

where $\beta = 1/k_B T$ and $L = 0, 1, \ldots$, with $g_0 = 1/2 + \langle s_z\rangle$ the intensive magnetization. We then obtain

$$p_L^\pm = \big(g_0 - \tfrac{1}{2} \pm \tfrac{1}{2}\big)^2 - g_L^2, \quad p_L = g_0 - g_0^2 + g_L^2, \quad (22)$$

$$\alpha_L = \tfrac{1}{2}\mathrm{Det}(A_L), \quad A_{ij} = 2g_{i-j+1} - \delta_{i,j-1}, \quad (23)$$

with A_L the first $L \times L$ block of the matrix of elements A_{ij} $(i, j = 1, \ldots, L)$. Thus, $\alpha_1 = g_1, \alpha_2 = g_2(1 - 2g_0) + 2g_1^2$, etc.

Ground-state results. At $T = 0$, all correlations vanish for $|B| > J$, where the ground state is fully aligned along z ($\alpha_L = 0$, $p_L^+ = 1 \forall\ L$). For $|B| < J$, we obtain instead

$$g_L = \frac{\sin(\omega L)}{L\pi}, \quad \omega = \arccos(B/J), \quad (24)$$

with $g_0 = \omega/\pi$.

Results for I_2, I_1, D and the eigenvalues of ρ_L are shown in Figs. 1 and 2 for $L = 1$ and 3. It is first verified that while the minimum quantum discord corresponds to $D^\perp\ \forall\ |B| < J$, the minimum geometric discord I_2 exhibits, for decreasing B, the expected sharp $I_2^z \rightarrow I_2^\perp$ transition. Moreover, for $L = 1$, this transition takes place *exactly at the point where the Bell state $|\Psi_+\rangle$ becomes dominant* in ρ_L, i.e., $B_c^L = B_t^L$. Remarkably, for $L = 1$ this exact coincidence occurs *at both zero and finite temperatures*, as follows from Eqs. (22) and (23): In this case $\alpha_1 = g_1$ and the crossing condition (14), $\alpha_1 = p_1^- - p_1$, implies

$$g_1 = \tfrac{1}{2} - g_0 \quad (25)$$

at this point. In such a case $p_1 - p_1^+ = p_1^- - p_1 = \alpha_1$, so that $\alpha_1^c = \alpha_1^t$ [Eq. (15)] and hence $B_t^L = B_c^L$ for $L = 1$. At $T = 0$ we have, explicitly,

$$\alpha_1 = \frac{\sin\omega}{\pi} = \frac{\sqrt{1 - B^2/J^2}}{\pi}, \quad (26)$$

and this transition occurs at $B_t \approx 0.67J$, i.e., $\sin\omega = \pi/2 - \omega$, corresponding to an intensive magnetization $\langle s_z\rangle \approx -0.235$. It is also seen that $I_2 \geqslant C^2\ \forall\ B$, i.e., the geometric discord remains larger than the corresponding entanglement monotone.

The behavior of the information deficit I_1 is similar, except that the previous transition is smoothed through a small *crossover region* $0.55 \lesssim B/J \lesssim 0.67$ where an *intermediate* measurement ($0 < \gamma < \pi/2$) provides the actual minimum: As B decreases, the minimizing angle γ increases smoothly from 0 to $\pi/2$ in this interval.

For higher separations, the behavior is similar except that values of I_f and D are lower and the transition field B_t^L is shifted towards lower fields, in agreement with the decrease of the field B_c^L where $|\Psi_+\rangle$ becomes dominant, as seen in Fig. 2

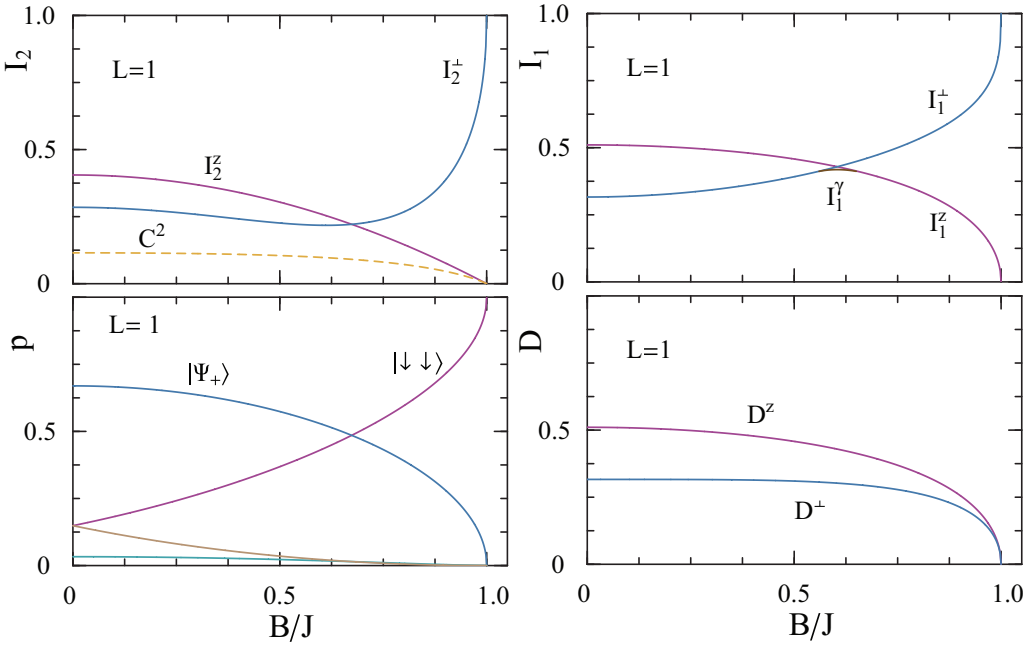

FIG. 1. (Color online) Results for the geometric discord I_2 (top left), the information deficit I_1 (top right), the quantum discord D (bottom right), and the eigenvalues of the reduced density matrix ρ_L (bottom left) for a pair of contiguous spins ($L = 1$) in the ground state of the XX chain in the thermodynamic limit, as a function of the scaled transverse field. Superscripts z and $\perp$ denote the results for spin measurements parallel and perpendicular to the field. In the top right panel, the intermediate minimum I_1^{γ} in the small crossover region is also shown. The dashed line in the top left panel depicts the square of the concurrence C. The minimum I_ν ($\nu = 1,2$) corresponds to $I_\nu^{\perp}$ essentially in the region where the dominant eigenvector of ρ_L is the Bell state $|\Psi_+\rangle$.

for $L = 3$. B_t^L remains close to B_c^L but the agreement is not exact. The quantum discord continues to be minimized by a perpendicular measurement $\forall\, |B| < J$. Notice that in this case the concurrence is very small and nonzero just in the vicinity of $B = J$, whereas all I_f and D remain nonzero $\forall\ |B| < J$, $\forall\ L$.

Results for large separations $L \gtrsim 3$ can be fully understood with the small α_L,δ expressions (17), (18), and (20). For large L, we may neglect g_L in $p_L^{\pm}$ and p_L, in which case $p_L \approx \sqrt{p_L^+ p_L^-} = \frac{\omega}{\pi}(1 - \frac{\omega}{\pi})$, while

$$\alpha_L = \eta_L/\sqrt{L}, \tag{27}$$

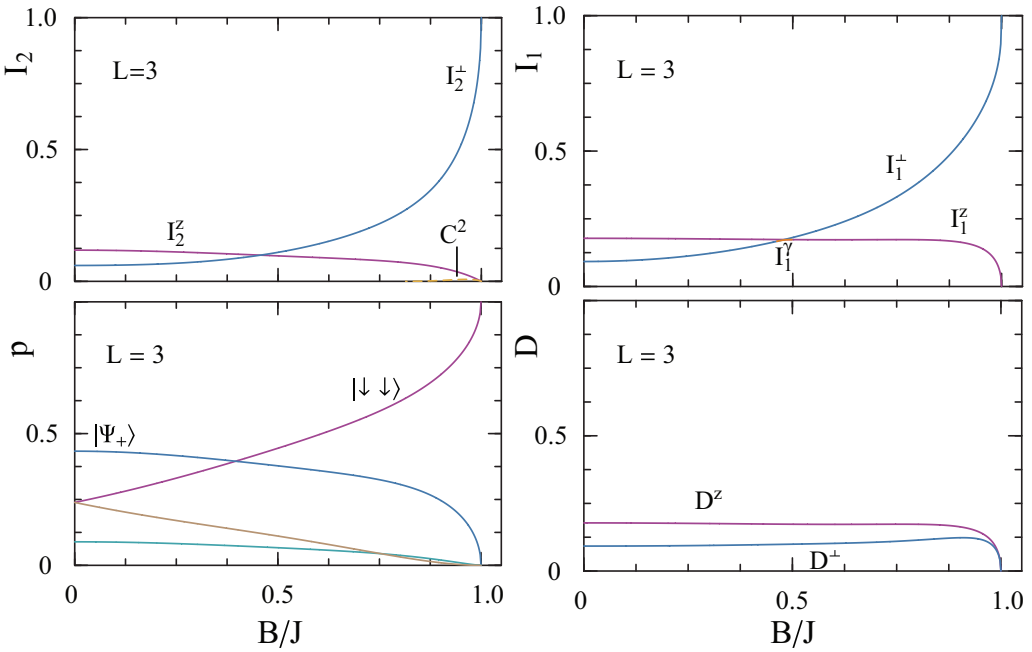

FIG. 2. (Color online) The same quantities of Fig. 1 for third neighbors ($L = 3$).

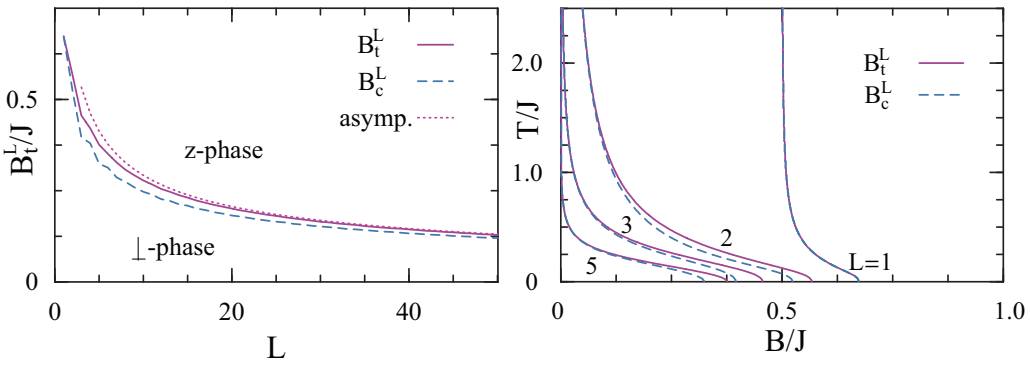

FIG. 3. (Color online) Left: The $T = 0$ transition field B_t^L where the measurement minimizing the geometric discord I_2 changes from perpendicular to parallel, as a function of the separation L (solid line), together with the $T = 0$ field B_c^L where the dominant eigenvector of ρ_L changes from a Bell state to an aligned state (dashed line). Both fields coincide for $L = 1$ and $L \to \infty$. The asymptotic result (30) for large L is also depicted (dotted line). Right: The transition fields $B_t^L(T)$ of the geometric discord at finite temperatures, for $L = 1$, 2, 3, and 5, such that $I_2 = I_2^\perp$ (I_2^z) for $B < B_t^L(T)$ [$> B_t^L(T)$]. Dashed lines depict again the fields $B_c^L(T)$ below which the Bell state is the dominant eigenvector of ρ_L. For $L = 1$, both fields coincide exactly $\forall\, T$, approaching $J/2$ for high T, whereas for $L \geqslant 2$ they merge for high T, vanishing as $(J/T)^{L-1}$ [Eq. (35)].

with η_L approaching a *finite* value as L increases ($\eta_L \to 0.294$ at $B = 0$, decreasing with increasing B). For sufficiently large L, Eq. (17) then leads to

$$I_f = I_f^z \approx k_f \eta_L^2 / L\,, \quad |B| > B_t^L, \tag{28}$$

with $k_f = |f''(p_L)|$ ($k_f = 4$ in I_2 and $\frac{1}{p_L \ln 2}$ in I_1). Hence, *all I_f's decrease as L^{-1} for increasing separations L*.

For large L, the transition field B_t^L becomes small, so that for $|B| < B_t^L$ we may employ the lower row of Eq. (18), with $\delta \approx -B/(\pi J)$, since (24) implies here $\omega \approx \pi/2 - B/J$ and hence $p_L^\pm \approx \frac{1}{4} \mp B/(\pi J)$:

$$I_f = I_f^\perp \approx \tfrac{1}{2} k_f \left[\eta_L^2/L + B^2/(\pi J)^2\right], \quad |B| < B_t \tag{29}$$

where $k_f = |f''(1/4)|$ and

$$B_t^L \approx \pi \eta_L J/\sqrt{L}, \tag{30}$$

as determined from the condition $I_f^\perp = I_f^z$ [$\eta_L \approx 0.294$ in Eqs. (29) and (30)]. This last equation coincides for large L with the condition $\alpha_L = p_L^- - p_L$ [Eq. (14)], so that in this limit $B_t^L = B_c^L$, as seen in the left panel of Fig. 3: The field (30) also determines the onset as B decreases of $|\Psi^+\rangle$ as the dominant eigenstate of ρ_L. This field decreases then as $L^{-1/2}$.

On the other hand, the quantum discord exhibits no transition: it is verified that $D = D^\perp\ \forall\ B, L$. Its expression for large L can be obtained directly from Eq. (20) and implies $D \propto L^{-1}$ for large L, like I_f:

$$D = D^\perp \approx k_D\, \eta_L^2 / L, \tag{31}$$

where $k_D = \frac{1}{\ln 2}\left(\frac{1}{p_L} - \frac{\operatorname{arctanh} 2\delta}{\delta}\right)$ with $\delta = \omega/\pi - 1/2$. For $B \to 0$, $\delta \to 0$ while $p_L \to 1/4$, and $D^\perp \to I_1^\perp$.

We finally notice that for $B \to J$, Eq. (24) leads to $\omega \approx \sqrt{2(1 - B/J)}$, and hence $\alpha_L \approx g_L \approx \omega/\pi\ \forall\, L$ at leading order. We then obtain the common L-independent limits

$$I_2 \approx 8(1 - B/J)/\pi^2\,, \quad I_1 \approx \sqrt{I_2} \quad (B \to J) \tag{32}$$

with $D \approx I_1$ at leading order. The independence of separation for $B \to J$ is verified and easily understood in the finite case (see next section).

Finite temperatures. As T increases, α_L decreases for fields $|B| < J$ (actually $|B| < J - \varepsilon_L$, with ε_L small), implying the decrease of all quantum correlations in this region. Nonetheless, while the concurrence (and hence entanglement) terminates at a finite T [39], the quantum discord and all I_f's vanish only asymptotically for high T. In addition, for $T > 0$ a small but finite value of D and I_f will also arise for $B > J$ (Fig. 4), as correlated excited states become accessible.

Setting $k_B = 1$, at high temperatures $T \gg \mathrm{Max}[J, B]$, Eqs. (22) and (23) lead to

$$g_0 \approx \frac{1}{2} - \frac{B}{4T}, \quad g_1 \approx \frac{J}{8T},$$

with $g_L = O(T^{-3})$ or higher for $L \geqslant 2$. Hence, in this limit we obtain, at leading nonzero order,

$$p_L^\pm \approx \tfrac{1}{4}(1 \mp B/T), \quad p_L \approx \tfrac{1}{4}, \quad \alpha_L \approx \tfrac{1}{2}(J/4T)^L, \tag{33}$$

implying that we may directly apply Eqs. (18) and (20). Therefore, I_f and D will vanish *exponentially* with increasing L, i.e., $I_f, D \propto (T/J)^{-2L}$. Nonetheless, for all I_f's there is still a transition field $B_t^L\ \forall\, T$ such that $I_f^\perp < I_f^z$ for $|B| < B_t^L$, with B_t^L decreasing with increasing T and approaching the field B_c^L for the onset of $|\Psi_+\rangle$ as the dominant eigenstate of ρ_L. The final result for high T derived from Eq. (18) is

$$I_f = \begin{cases} I_f^z \approx \frac{k_f}{4}\left(\frac{J}{4T}\right)^{2L}, & |B| > B_t^L \\ I_f^\perp \approx \frac{k_f}{2}\left(\frac{1}{4}\left(\frac{J}{4T}\right)^{2L} + \frac{B^2}{(4T)^2}\right), & |B| < B_t^L \end{cases} \tag{34}$$

where $k_f = |f''(p_L)| \approx |f''(1/4)|$ and

$$B_t^L \approx \frac{J}{2}\left(\frac{J}{4T}\right)^{L-1}, \tag{35}$$

as determined from the condition $I_f^\perp = I_f^z$, which coincides in this limit with that derived from the crossing condition (14). Hence, for first neighbors ($L = 1$) B_t^L approaches for high T the *finite* limit $J/2$, whereas for $L \geqslant 2$ it decreases as

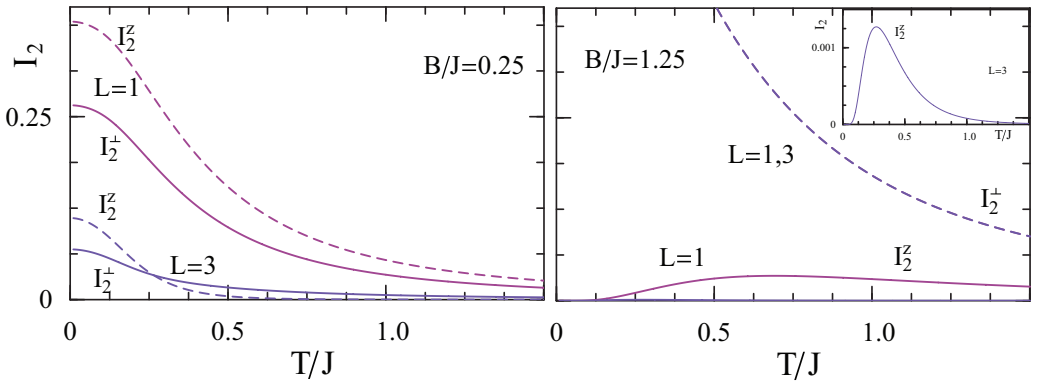

FIG. 4. (Color online) The geometric discord I_2 vs temperature at fixed field, for first and third neighbors. At fields $B < B_c = J$ (left panel), I_2 decreases with increasing T and a transition $I_2^{\perp} \to I_2^{z}$ can take place, as seen here for $L = 3$. For $B > B_c$, $I_2 = I_2^{z}$ first increases at low T, although this revival becomes very small as L increases, as seen in the inset for $L = 3$. For high T, $I_2 \propto (T/J)^{-2L}$ [Eq. (34)].

$(J/T)^{L-1}$, as verified in the right panel of Fig. 3 for I_2. In this limit, the transition fields B_t^L approach $B_c^L \; \forall \; I_f$. For lower T, they remain quite close. It is also seen in Fig. 3 that in the case of I_2, $B_t^L = B_c^L \; \forall \; T$ for $L = 1$, as previously demonstrated.

In contrast, $D = D^{\perp} \; \forall \; B,T$, with [Eq. (20)]

$$D^{\perp} \approx \frac{k_D}{4}\left(\frac{J}{4T}\right)^{2L} \tag{36}$$

for high T, where $k_D \approx \frac{2}{\ln 2}$. Again, $D^{\perp} \approx I_1^{\perp}$ for $B \to 0$.

We finally notice that for $T > 0$ and strong fields $B \gg J,T$, we have

$$g_L \approx \frac{e^{-\beta B}}{\pi}\int_0^{\pi} e^{\beta J\cos\omega}\cos(L\omega)d\omega = e^{-\beta B} I_L(\beta J),$$

where $I_L(x)$ denotes the modified Bessel function of the first kind [$I_L(x) \approx e^x/\sqrt{2\pi x}$ for $x \to \infty$ while $I_L(x) \approx (x/2)^L/L!$ for $x \to 0$]. Hence, in this limit, g_L decreases exponentially with the field, with $p_L \approx g_0$ and $\alpha_L \approx g_L$. The geometric discord then becomes

$$I_2 \approx 4e^{-2B/T} I_L^2(J/T), \tag{37}$$

decreasing as $e^{-2B/T}$ for strong fields and also quite fast with separation if $B \gg T \gg J$ [$I_L(J/T) \approx (J/2T)^L/L!$]. On the other hand, I_1 and D will decrease for strong fields as α_L ($\propto e^{-B/T}$).

C. Finite case

In a finite chain, the exact ground state has a definite discrete magnetization M. Therefore, it will exhibit N transitions $M \to M+1$ as the field decreases from above $B_c = J$, starting at $M = -N/2$ for $B > B_c$. In the cyclic case, the critical fields are given by [39]

$$B_k = J\frac{\cos[\pi(k-1/2)/N]}{\cos[\pi/(2N)]}, \quad k = 1,\ldots,N \tag{38}$$

such that $M = k - N/2$ for $B_{k+1} < B < B_k$, with $B_1 = J$, $B_N = -J$. For $N \to \infty$, Eq. (38) reduces to Eq. (24) ($B = J\cos\omega$, with $\omega/\pi = k/N = 1/2 + M/N$). Details of the exact calculation for the finite case at 0 and finite T are given in the Appendix.

Accordingly, all measures I_f and D will exhibit at $T = 0$ a stepwise behavior, starting from 0 for $B > B_c$, which can be appreciated in Fig. 5 and which is centered around the result for the thermodynamic limit (also depicted for $L = 1,2,3$ and $N/2$) for $L \lesssim N/4$. Just for large $L \gtrsim N/4$, the finite result becomes larger. In contrast, the concurrence is nonzero for large L just in the immediate vicinity of $B_c = J$.

Actually, as shown in the insets of Fig. 5, all measures I_f, D, and C acquire a *common value for all separations* L for $B \to J$, i.e., in the first interval $B_2 < B < B_1$, where $M = -N/2 + 1$ and the ground state is the W state

$$|\Psi_0\rangle = \frac{1}{\sqrt{N}}(|\uparrow\downarrow\downarrow\cdots\rangle + \cdots + |\cdots\downarrow\downarrow\uparrow\rangle).$$

This state leads to an L-independent rank-2 reduced state ρ_L, with $p_L^+ = 0$, $p_L^- = 1 - 2/N$, and $p_L = \alpha_L = 1/N$ in (10). For such state we obtain, if $N \geqslant 4$,

$$I_2 = I_2^z = \frac{4}{N^2} = C^2, \;\; I_1 = I_1^z = \sqrt{I_2}, \tag{39}$$

in agreement with the thermodynamic limit result (32) [for large N, the second critical field is $B_2 \approx J(1 - \frac{\pi^2}{N^2})$ and hence, $\frac{8}{\pi^2}(1 - \frac{B}{J}) \approx \frac{4}{N^2}$ if $B = \frac{B_1+B_2}{2}$]. Note that for this state, $\alpha_L \leqslant \alpha_c = p_L^- - p_L \; \forall \; N \geqslant 4$ (just for $N = 3$, where $\alpha_L > \alpha_c$, a perpendicular measurement is preferred in both I_2 and I_1). In contrast, D is minimized by a perpendicular measurement $\forall N$, with

$$D^{\perp} \approx \frac{2}{N} - \frac{1}{N^2}\log_2(N/e), \tag{40}$$

for large N (although $D^{\perp} \approx D^z = I_1^z$ at leading order).

For lower fields, it is seen that for small $L \geqslant 2$, I_2 is maximum at the parallel-to-perpendicular transition. Such maximum becomes flattened in I_1 and is absent in the quantum discord D since the latter is minimized by a perpendicular measurement $\forall \; B < J$ and L. For $L > 1$, its maximum is attained in the vicinity of $B_c = J$.

The minimizing angles for I_2 and D in the finite case of Fig. 5 are depicted in Fig. 6. For I_2, it exhibits the sharp transition from $\gamma = 0$ (z phase) to $\gamma = \pi/2$ ($\perp$ phase) as B decreases, which now occurs *at one of transition fields* (38) ($B_t^L = B_k$ for some L-dependent k). For $L = 1$, the measurement transition signals exactly that ground-state transition $M \to M+1$ where ρ_L changes its dominant eigenstate, as clearly depicted in the top right panel of Fig. 6 [where

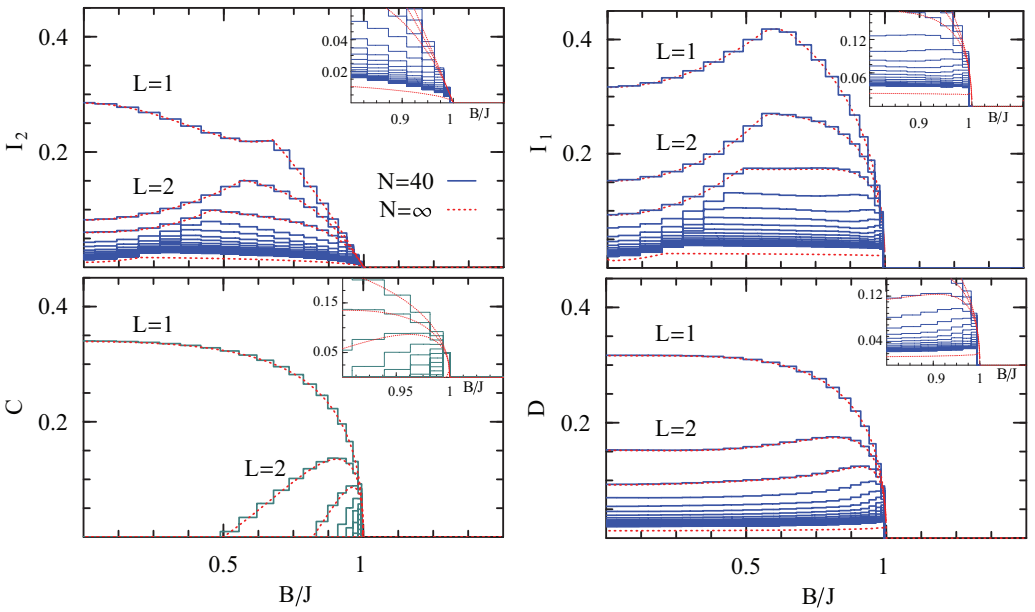

FIG. 5. (Color online) The minimum geometric discord I_2 (top left), information deficit I_1 (top right), and quantum discord D (bottom right) for spin pairs with separation $L = 1, \ldots, N/2$ in the ground state of a finite cyclic chain of $N = 40$ spins as a function of the scaled transverse magnetic field. For reference, the concurrence (bottom left) is also depicted. The dotted lines depict the thermodynamic limit for separations $L = 1$, 2, 3 and $N/2$. In each panel, the inset depicts the vicinity of the critical field $B_c = J$, where all curves reach a common value for all separations L [Eqs. (39) and (40)].

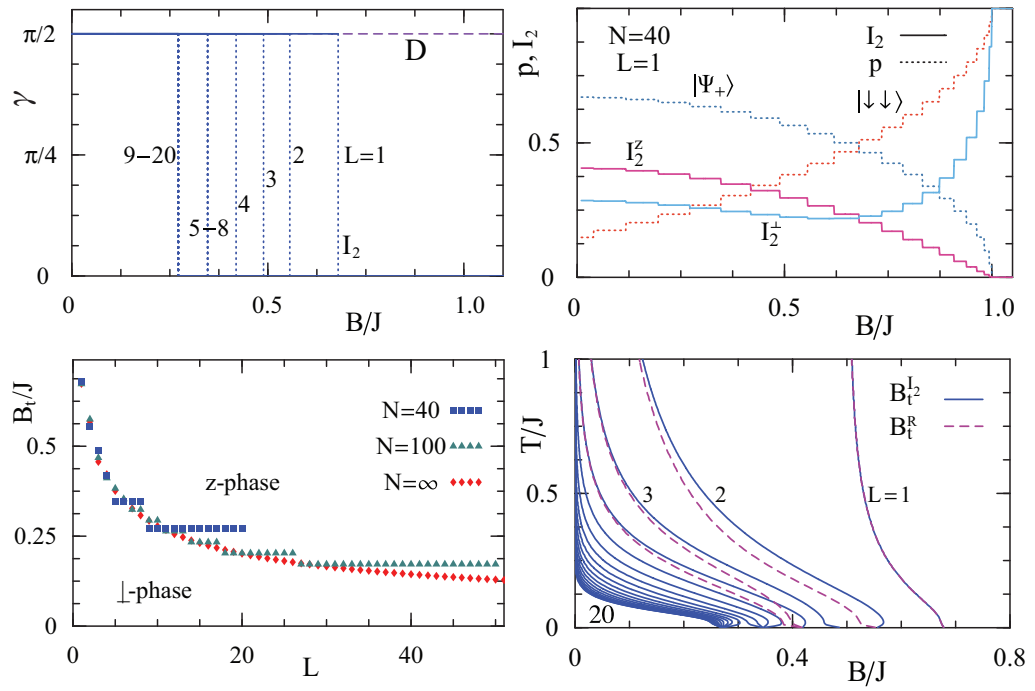

FIG. 6. (Color online) Top: Left: The minimizing angle for the geometric discord I_2 as a function of the magnetic field for spin pairs with separations $L = 1, \ldots, N/2$, in the finite chain of Fig. 5. Dotted lines indicate the sharp $\perp \to z$ transitions for different L. No transition occurs in the quantum discord D (dashed line), where $\gamma = \pi/2 \; \forall \; B$ and L. Right: Results for the geometric discord $I_2^{\perp}$ and I_2^{z} (solid lines) for $N = 40$ and $L = 1$, together with the two dominant eigenvalues of ρ_1 (dotted lines). Both cross at the same step. Bottom: Left: Exact transition fields B_t^L delimiting the $\perp$ and z phases of I_2 at $T = 0$ for $N = 40$, 100, and the thermodynamic limit. Right: The geometric discord "phase" diagram in the finite chain of $N = 40$ spins, for all separations $L = 1, \ldots, N/2$ (solid lines). The z ($\perp$) phase lies to the right (left) of these curves. Dashed lines depict the fields $B_c^L(T)$ for $L \leqslant 4$, below which the Bell state becomes dominant in ρ_L.

it corresponds to $k = 11$ in (38)], while for larger L both transitions are very close. As seen in the left panels of Fig. 6, as L increases the transition fields for different L begin to merge, coinciding for large $L \gtrsim N/4$, while as N increases they approach the thermodynamic limit result for $L \lesssim N/4$, becoming then constant. A similar picture is obtained for the minimizing angle of I_1, although in this case the measurement transition can occur in two or three "steps," reminiscent of the smoothed transition of the thermodynamic limit.

The bottom right panel in Fig. 6 depicts the finite-temperature geometric discord "phase" diagram according to the minimizing measurement for $N = 40$ spins (fields B_t^L), together with the fields B_c^L where the dominant eigenstate changes from the Bell state to an aligned state, for all separations $L = 1, \ldots, N/2$. For $L = 1$, there is again almost exact coincidence between both fields for all T since the deviation from the thermodynamic limit condition (25) is small. For larger L, the agreement is not exact for low T, but they become again coincident for high temperatures $\forall L$, where deviations from the thermodynamic limit results become small.

IV. CONCLUSIONS

We have examined the behavior of discord-type measures of quantum correlations for the case of spin pairs in the cyclic *XX* chain. Their behavior is substantially different from that of the pair entanglement, acquiring at $T = 0$ nonzero values for all pair separations L if $B < B_c$ and decaying only as L^{-1} for large L. Moreover, they remain nonzero for all temperatures, decaying as T^{-2L} for sufficiently high T. Thus, they all exhibit the same "universal" asymptotics, independently of the particular choice of entropic function in I_f. It can then be most easily accessed through the geometric discord, which offers the simplest evaluation. The ensuing picture is, consequently, quite different from that exhibited by the pair entanglement [39], which, although reaching full range in the immediate vicinity of B_c, is appreciable just for the first few neighbors, as seen in Fig. 5, and strictly vanishes beyond a low-limit temperature. Hence, critical systems such as the *XX* chain seem to offer vast possibilities for discord-type quantum correlations between close or distant pairs.

The second important result is that in spite of the similar behavior, these measures exhibit substantial differences in the minimizing local spin measurement that defines them. The quantum discord, which minimizes a conditional entropy, always prefers here measurements along a direction orthogonal to the transverse field, even if correlations are weak (i.e., large L, high T, or strong fields B if $T > 0$). The information-deficit-type measures, which evaluate the minimum global information loss due to such measurement and include the geometric discord and the one-way information deficit, exhibit instead a transition in the optimum measurement, from perpendicular to parallel to the field as the latter increases, present for all pair separations and at all temperatures. Such difference was previously observed in certain two-qubit and two-qutrit states [25,49].

In the present model, such behavior is a signature of the transition exhibited by the dominant eigenstate of the reduced state of the pair, which changes from a maximally entangled state to a separable state in the immediate vicinity of the measurement transition. Hence, the latter reveals an actual relevant change in the structure of the reduced state. Moreover, for contiguous pairs and in the case of the geometric discord, both transitions occur *exactly* at the same field, at all temperatures. For general separations, there is also exact agreement between both fields at high T, for *all measures* I_f. In the finite chain, the $T = 0$ measurement transition coincides of course with one of the ground-state magnetization transitions $M \to M + 1$. These results indicate that the "least disturbing" local measurement optimizing these quantities can be significantly different from that minimizing the quantum discord, even though they coincide exactly in some regimes, being essentially affected by the main component of the reduced state. Its changes can then be used to characterize different quantum regimes, even when entanglement is absent.

ACKNOWLEDGMENT

The authors acknowledge support from CONICET (L.C., N.C.) and CIC (R.R.) of Argentina.

APPENDIX: EXACT SOLUTION OF THE CYCLIC CHAIN

We give here a brief summary of the method employed for obtaining the exact solution of the cyclic *XX* chain for both finite N and the thermodynamic limit, at both 0 and finite T [39]. Through the Jordan-Wigner transformation [41], and for each value $\sigma = \pm 1$ of the S_z parity $P_z = \exp[i\pi(S_z + N/2)]$, the *XX* Hamiltonian can be mapped exactly to the fermionic Hamiltonian

$$H_\sigma = \sum_{j=1}^{N} B\left(c_j^\dagger c_j - \frac{1}{2}\right) - \frac{1}{2} J(1 - \delta_{jN}\delta_{\sigma 1})\left(c_j^\dagger c_{j+1} + c_{j+1}^\dagger c_j\right), \quad \text{(A1)}$$

where $N + 1 \equiv 1$ and $c_j, c_j^\dagger$ denote fermion annihilation and creation operators. Equation (A1) can be solved exactly through a discrete Fourier transform $c_j^\dagger = \frac{1}{\sqrt{N}} \sum_{k \in K_\sigma} e^{i\omega_k j} c_k'^\dagger$ to fermion operators c_k', where $\omega_k = 2\pi k/N$ and k is *half-integer (integer)* for $\sigma = 1$ (-1), i.e., $K_\sigma = \{-[\frac{N}{2}] + \delta_\sigma, \ldots, [\frac{N-1}{2}] + \delta_\sigma\}$ with $[\cdots]$ the integer part and $\delta_1 = \frac{1}{2}$, $\delta_{-1} = 0$. We then obtain

$$H_\sigma = \sum_{k \in K_\sigma} \lambda_k \left(c_k'^\dagger c_k' - \frac{1}{2}\right), \quad \lambda_k = b - v\cos\omega_k. \quad \text{(A2)}$$

The 2^N energies are then $\sum_{k \in K_\sigma} \lambda_k (N_k - 1/2)$, where $N_k = 0, 1$ and $\sigma = (-1)^{\sum_k N_k}$. The single-fermion energies λ_k depend on the global parity σ and are degenerate ($\lambda_k = \lambda_{-k}$) for $|k| \neq 0, N/2$. A careful comparison of the ensuing levels leads to the critical fields (38).

The exact partition function Z of the spin system corresponds to the full grand-canonical ensemble of the fermionic representation. However, due to the parity dependence of the latter, this requires a (fermion) *number parity projected statistics* [39]. Z can then be written as a sum of partition functions for each parity,

$$Z = \mathrm{Tr} \sum_{\sigma = \pm 1} P_\sigma e^{-\beta H_\sigma} = \frac{1}{2} \sum_{\sigma = \pm 1} \left(Z_0^\sigma + \sigma Z_1^\sigma\right), \quad \text{(A3)}$$

where $P_\sigma = \frac{1}{2}(1+\sigma P_z)$ is the projector onto parity σ and $Z_\nu^\sigma = e^{\beta BN/2}\prod_{k\in K_\sigma}[1+(-1)^\nu e^{-\beta\lambda_k}]$ for $\nu = 0,1$. The thermal average of an operator O can then be written as

$$\langle O\rangle = \frac{1}{2}Z^{-1}\sum_{\sigma=\pm1}\left(Z_0^\sigma\langle O\rangle_0^\sigma + \sigma Z_1^\sigma\langle O\rangle_1^\sigma\right), \qquad \text{(A4)}$$

where $\langle O\rangle_\nu^\sigma = (Z_\nu^\sigma)^{-1}\mathrm{Tr}\,[P_z^\nu e^{-\beta H_\sigma}O]$. For many-body fermion operators O, the thermal version of Wick's theorem *can not* be applied in the final average (A4), but it *can* be applied for evaluating the partial averages $\langle O\rangle_\nu^\sigma$, in terms of the basic contractions ($L = |i-j|$)

$$g_L \equiv \langle c_i^\dagger c_j\rangle_\nu^\sigma = N^{-1}\sum_{k\in K_\sigma}\langle c_k'^\dagger c_k'\rangle_\nu^\sigma\cos(L\omega_k), \qquad \text{(A5)}$$

where $\langle c_k'^\dagger c_k'\rangle_\nu^\sigma = [1+(-1)^\nu e^{\beta\lambda_k}]^{-1}$. As $s_{iz} = c_i^\dagger c_i - \frac{1}{2}$, this leads to $\langle s_{iz}\rangle_\sigma^\nu = g_0 - \frac{1}{2}$ and

$$\left\langle\left(s_{iz}+\tfrac{1}{2}\right)\left(s_{jz}+\tfrac{1}{2}\right)\right\rangle_\nu^\sigma = g_0^2 - g_L^2, \quad \langle s_{i+}s_{j-}\rangle_\nu^\sigma = \tfrac{1}{2}\mathrm{Det}(A_L),$$

where $s_{j\pm} = s_{jx} \pm i s_{jy}$ and A_L is the $L\times L$ matrix of elements $(A_L)_{ij} = 2g_{i-j+1} - \delta_{i,j-1}$. All elements in (10) can then be analytically evaluated.

For $N\to\infty$ and finite separations L, we can ignore parity effects and directly employ Wick's theorem in terms of the final averages $g_L = \langle c_i^\dagger c_j\rangle$, with sums over k replaced by integrals over $\omega \equiv \omega_k$. This leads to Eqs. (21)–(23). When the ground state is nondegenerate, Eqs. (22) and (23) can also be applied for *finite* N in the $T\to 0$ limit, using the exact contractions $g_L \equiv \langle c_i^\dagger c_j\rangle_0 = \frac{1}{N}\sum_{k\in K_\sigma} N_k\cos(L\omega_k)$, with $N_k = 0,1$ the occupation of level k.

[1] K. Modi *et al.*, Rev. Mod. Phys. **84**, 1655 (2012).
[2] R. F. Werner, Phys. Rev. A **40**, 4277 (1989).
[3] E. Knill and R. Laflamme, Phys. Rev. Lett. **81**, 5672 (1998).
[4] A. Datta, S. T. Flammia, and C. M. Caves, Phys. Rev. A **72**, 042316 (2005).
[5] R. Jozsa and N. Linden, Proc. R. Soc. Lon. A **459**, 2011 (2003); G. Vidal, Phys. Rev. Lett. **91**, 147902 (2003).
[6] H. Ollivier and W. H. Zurek, Phys. Rev. Lett. **88**, 017901 (2001).
[7] L. Henderson and V. Vedral, J. Phys. A: Math. Gen. **34**, 6899 (2001); V. Vedral, Phys. Rev. Lett. **90**, 050401 (2003).
[8] W. H. Zurek, Phys. Rev. A **67**, 012320 (2003).
[9] A. Datta, A. Shaji, and C. M. Caves, Phys. Rev. Lett. **100**, 050502 (2008).
[10] A. Datta and S. Gharibian, Phys. Rev. A **79**, 042325 (2009).
[11] A. Shabani and D. A. Lidar, Phys. Rev. Lett. **102**, 100402 (2009).
[12] K. Modi, T. Paterek, W. Son, V. Vedral, and M. Williamson, Phys. Rev. Lett. **104**, 080501 (2010).
[13] A. Ferraro, L. Aolita, D. Cavalcanti, F. M. Cucchietti, and A. Acín, Phys. Rev. A **81**, 052318 (2010).
[14] F. F. Fanchini, M. F. Cornelio, M. C. de Oliveira, and A. O. Caldeira, Phys. Rev. A **84**, 012313 (2011).
[15] M. Horodecki, P. Horodecki, R. Horodecki, J. Oppenheim, A. Sen(De), U. Sen, and B. Synak-Radtke, Phys. Rev. A **71**, 062307 (2005); J. Oppenheim, M. Horodecki, P. Horodecki, and R. Horodecki, Phys. Rev. Lett. **89**, 180402 (2002).
[16] A. Streltsov, H. Kampermann, and D. Bruß, Phys. Rev. Lett. **106**, 160401 (2011).
[17] B. Dakić, V. Vedral, and C. Brukner, Phys. Rev. Lett. **105**, 190502 (2010).
[18] R. Rossignoli, N. Canosa, and L. Ciliberti, Phys. Rev. A **82**, 052342 (2010).
[19] V. Madhok and A. Datta, Phys. Rev. A **83**, 032323 (2011).
[20] D. Cavalcanti, L. Aolita, S. Boixo, K. Modi, M. Piani, and A. Winter, Phys. Rev. A **83**, 032324 (2011).
[21] M. Piani, S. Gharibian, G. Adesso, J. Calsamiglia, P. Horodecki, and A. Winter, Phys. Rev. Lett. **106**, 220403 (2011).
[22] D. Girolami and G. Adesso, Phys. Rev. Lett. **108**, 150403 (2012).
[23] T. Tufarelli, D. Girolami, R. Vasile, S. Bose, and G. Adesso, Phys. Rev. A **86**, 052326 (2012).
[24] B. Bellomo *et al.*, Phys. Rev. A **85**, 032104 (2012); B. Bellomo, R. Lo Franco, and G. Compagno, *ibid.* **86**, 012312 (2012); R. Lo Franco *et al.*, *ibid.* **85**, 032318 (2012).
[25] R. Rossignoli, N. Canosa, and L. Ciliberti, Phys. Rev. A **84**, 052329 (2011).
[26] R. Dillenschneider, Phys. Rev. B **78**, 224413 (2008).
[27] M. S. Sarandy, Phys. Rev. A **80**, 022108 (2009).
[28] J. Maziero, H. C. Guzman, L. C. Céleri, M. S. Sarandy, and R. M. Serra, Phys. Rev. A **82**, 012106 (2010).
[29] T. Werlang and G. Rigolin, Phys. Rev. A **81**, 044101 (2010).
[30] L. Ciliberti, R. Rossignoli, and N. Canosa, Phys. Rev. A **82**, 042316 (2010).
[31] T. Werlang, C. Trippe, G. A. P. Ribeiro, and G. Rigolin, Phys. Rev. Lett. **105**, 095702 (2010); T. Werlang, G. A. P. Ribeiro, and G. Rigolin, Phys. Rev. A **83**, 062334 (2011).
[32] B.-Q. Liu, B. Shao, J.-G. Li, J. Zou, and L.-A. Wu, Phys. Rev. A **83**, 052112 (2011).
[33] Y. C. Li and H. Q. Lin, Phys. Rev. A **83**, 052323 (2011).
[34] N. Canosa, L. Ciliberti, and R. Rossignoli, Int. J. Mod. Phys. B **27**, 1345033 (2012).
[35] B. Tomasello *et al.*, Europhys. Lett. **96**, 27002 (2011); B. Çakmak, G. Karpat, and Z. Gedik, Phys. Lett. A **376**, 2982 (2012).
[36] S. Campbell *et al.*, New J. Phys. **15**, 043033 (2013); C. C. Rulli and M. S. Sarandy, Phys. Rev. A **84**, 042109 (2011).
[37] S. Sachdev, *Quantum Phase Transitions* (Cambridge University Press, Cambridge, UK, 1999).
[38] X. Wang, Phys. Rev. A **66**, 034302 (2002).
[39] N. Canosa and R. Rossignoli, Phys. Rev. A **75**, 032350 (2007).
[40] M. Fujinaga and N. Hatano, J. Phys. Soc. Jpn. **76**, 094001 (2007); W. Son *et al.*, Phys. Rev. A **79**, 022302 (2009).
[41] E. Lieb, T. Schultz, and D. Mattis, Ann. Phys. (NY) **16**, 407 (1961).
[42] A. De Pasquale and P. Facchi, Phys. Rev. A **80**, 032102 (2009).
[43] N. Canosa and R. Rossignoli, Phys. Rev. Lett. **88**, 170401 (2002).
[44] H. Wehrl, Rev. Mod. Phys. **50**, 221 (1978).
[45] V. Vedral, Rev. Mod. Phys. **74**, 197 (2002).
[46] S. Hill and W. K. Wootters, Phys. Rev. Lett. **78**, 5022 (1997); W. K. Wootters, *ibid.* **80**, 2245 (1998).

[47] P. Rungta and C. M. Caves, Phys. Rev. A **67**, 012307 (2003); P. Rungta, V. Buzek, C. M. Caves, M. Hillery, and G. J. Milburn, *ibid*. **64**, 042315 (2001).

[48] C. Tsallis, J. Stat. Phys. **52**, 479 (1988); *Introduction to Non-Extensive Statistical Mechanics* (Springer, New York, 2009).

[49] R. Rossignoli, J. M. Matera, and N. Canosa, Phys. Rev. A **86**, 022104 (2012).

[50] M. Ali, A. R. P. Rau, and G. Alber, Phys. Rev. A **81**, 042105 (2010); **82**, 069902(E) (2010).

[51] D. Girolami and G. Adesso, Phys. Rev. A **83**, 052108 (2011).